BOREAL ENVIRONMENT RESEARCH 28: 97–110
ISSN 1797-2469 (online)

Helsinki 25 May 2023

First total OH reactivity emission measurements from a Nordic wetland

Simon Schallhart[1)], Arnaud P. Praplan[1)], Toni Tykkä[1)], Nina Reijrink[2)], Jonathan Williams[2)], Hannele Hakola[1)] and Heidi Hellén[1)]

[1)] *Finnish Meteorological Institute, P.O. Box 503, 00101 Helsinki, Finland (*corresponding author's e-mail: simon.schallhart@fmi.fi)*
[2)] *Atmospheric Chemistry Department, Hahn-Meitner-Weg 1, Max Planck Institute for Chemistry, 55128 Mainz, Germany*

Received 11 Aug. 2022, final version received 14 Mar. 2023, accepted 15 Mar. 2023

Schallhart S., Praplan A.P., Tykkä T., Reijrink N., Williams J., Hakola H. & Hellén H. 2023: First total OH reactivity emission measurements from a Nordic wetland. *Boreal Env. Res.* 28: 97–110.

Volatile organic compounds (VOCs) are ever-present compounds in the air we breathe. They are emitted by natural and anthropogenic sources and are modified by atmospheric oxidants. VOCs affect air quality and human health, form and grow aerosol particles, and can impact Earth's radiative balance. Total hydroxyl radical (OH) reactivity measurements are a valuable tool for assessing the comprehensiveness of measured VOCs and can give valuable insights into in situ atmospheric chemistry. Especially in remote forested environments, missing or unaccounted for reactivity has been substantial, caused by either unmeasured primary emissions or secondary oxidation products. This study presents OH reactivity and VOC measurements over a Nordic, subarctic wetland in summer. Over half of the OH reactivity from emissions could not be attributed, while the remaining measured fraction is dominated by isoprene (42%), followed by sesquiterpenes (3%).

Introduction

Volatile organic compounds (VOCs) are emitted in large amounts into the atmosphere (> 1200 Tg/yr). They are mainly emitted from biogenic sources and can react with ozone (O_3), the hydroxyl radical (OH), or nitrate radical (NO_3) to form oxidized VOCs. By reacting with these atmospheric oxidants, they can affect the lifetime of greenhouse gases (e.g., methane) and form or grow aerosol particles, all of which can affect Earth's radiative balance (Kaplan *et al.* 2006, Lelieveld *et al.* 2016).

The number of different VOCs is vast: estimations for the number of individual VOCs in the atmosphere exceed one million for compounds of ten carbon atoms or less (Goldstein and Galbally 2007). Their concentrations vary over several orders of magnitude, and their atmospheric lifetimes can span from minutes to days. Measuring VOCs is thus challenging, as generally, only a fraction of those present in the air will be quantified, because of technical limitations of analytical methods.

One way of quantifying the fraction of VOCs not accounted for by measurements is to use total OH reactivity. By measuring the total OH reactivity of an air sample and comparing it with the calculated reactivity of the individually measured VOCs summed together, the missing reactivity can be quantified. In the case of a large missing reactivity, either a

Editor in charge of this article: Veli-Matti Kerminen

large number of moderately reactive VOCs or a few very reactive VOCs were not measured. When no missing reactivity is observed, most VOCs will have been measured or the missing VOCs are not very reactive. Overall, the average missing OH reactivity values in remote environments are around 50% (Ferracci *et al.* 2018). Particularly in forested regions, significant OH reactivity has been reported (Williams and Brune 2015, Nölscher *et al.* 2016), although more recent work has now closed the budget even in the rainforest (Pfannerstill *et al.* 2021).

This total OH reactivity can be measured by the comparative reactivity method (CRM), where pyrrole is used to measure the reactivity indirectly. This method has been known for over a decade (Sinha *et al.* 2008) and has been used in many measurements covering different ecosystems (Yang *et al.* 2016). The main suspects causing the missing reactivities are oxidation products or undetected biogenic primary emissions. By using enclosures, e.g., for a tree branch, the total OH reactivity of emissions can be studied to test that hypothesis. Enclosures are continuously flushed with clean air, free of VOCs and oxidants so that only the reactivity of primary emissions can be measured and compared to the OH reactivity expected from the known chemical composition of the emissions. Currently, only three studies have been published about OH reactivity of emissions, all of which investigate emissions from trees, and their range of missing reactivity lies between almost none to 84% (Kim *et al.* 2011, Nölscher *et al.* 2013, Praplan *et al.* 2020).

This study presents the total OH reactivity of emissions of a subarctic wetland, in Finnish Lapland. More than 50% of the global wetlands are located in the high northern latitudes (Davidson 2014) and are an essential part of the boreal landscape. Olefeldt *et al.* (2021) estimate that their Boreal–Arctic Wetland and Lake Dataset wetlands cover 3.18×10^6 km^2, 30% of the boreal forest cover (10.66×10^6 km^2). Wetlands are very vulnerable to changes in climate, and it is unclear if the thawing of the perma-frost soils will lead to more wetland areas (van der Kolk *et al.* 2016) or reduce them (Avis *et al.* 2011).

Experimental setup

Measurement site

The VOC emission measurements were conducted between 25 April and 2 August 2018 in the subarctic Lompolojänkkä fen (67.9973°N, 24.2095°E) in the Pallas-Yllästunturi National Park. An intensive air chemistry measurement campaign that included OH reactivity measurements of direct emissions was performed during the main growing season between 1 July and 2 August 2018. The open and mesotrophic sedge fen lies 269 m a.s.l. and has a relatively high water level, leading to a water-saturated peat level throughout most of the year. The vegetation height is about 40 cm, and the moss layer consists mainly of peat (*Sphagnum angustifolium, S. riparium, and S. fallax*) and brown mosses (*Warnstorfia exannulata*). A detailed description of the fen can be found in Aurela *et al.* (2015). During the intensive campaign, the average ambient air temperature was 19°C, varying between 1°C and 32°C, and the cumulated rainfall of the 33-day intensive campaign was 33.7 mm. The summer of 2018 was exceptionally hot and dry in Fennoscandia; Lompolojänkkä experienced 11% less precipitation than during the climatological normal from 1981–2010, and the average annual temperature was 1.8°C warmer (Rinne *et al.* 2020). However, the water table of the wetland was not affected by the missing precipitation.

Surrounding the wetland is coniferous forest, which consists of 72% Scots pine (*Pinus sylvestris*), 20% Norway Spruce (*Picea abies*), and the remaining 8% are deciduous trees (mainly *Betula pubescens*, *Populus tremula,* and *Salix spp*.).

Measurement setup

The setup used for the OH reactivity measurement (Fig. 1) consisted of a pump, which directed air through a dryer and a commercial zero air generator (HPZA-7000, Parker Hannifin Corporation) and then via fluorinated ethylene propylene (FEP) tubing (4 mm i.d.) to a 60 × 60 x 25 cm FEP soil chamber placed on

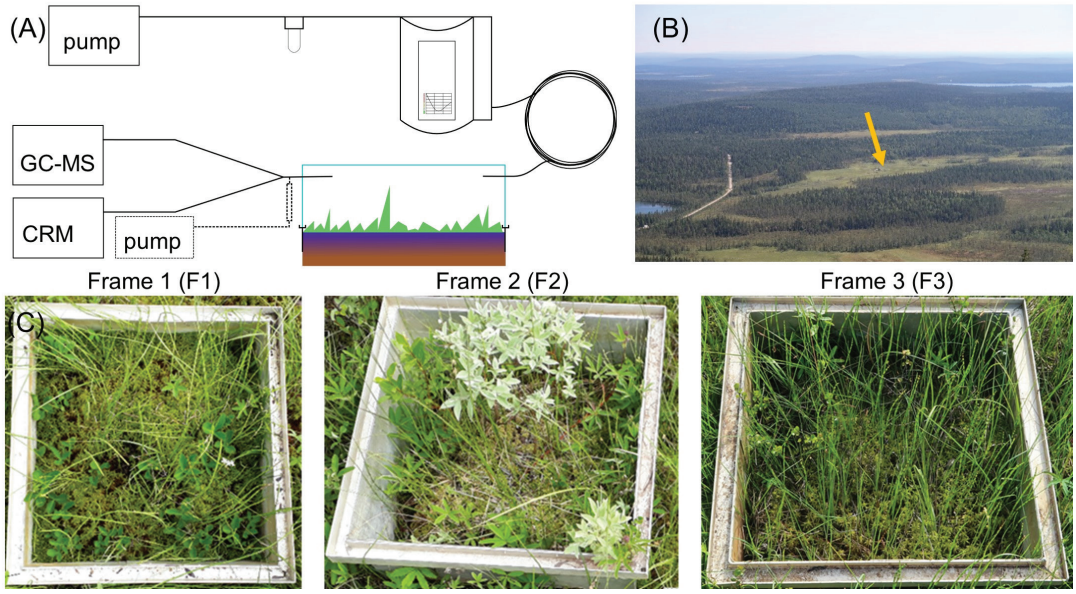

Fig. 1. (**A**) Schematic drawing of the setup used. The dashed pump and cartridge part was only used in the last measurement period. (**B**) Picture of the surrounding area of the measurement site (arrow). (**C**) Photos from the beginning of June 2018 showing the tree frames used in the measurements. (Photos taken from Hellén et al., 2020)

stainless steel frames. The frames were installed in the wetland 8 months before the start of the campaign. The clean airflow to the chamber varied between 4 and 6 L min^{-1} during the campaign.

Three frames were used (Fig. 1), all in the vicinity of the cottage where instrumentation for the campaign was installed. The vegetation in Frame 1 consisted of forbs (*Menyanthes trifoliate*, *Comarum palustre*, *Equisetum fluviatile*) and different sedges and sphagnum moss species. Frame 2's vegetation was dominated by two willow species (*Salix lapponum and Salix phylicifolia*), purple marshlocks (*Comarum palustre*), and various sedge and sphagnum moss species. The vegetation in Frame 3 consisted of different sedges and sphagnum moss species together a with smaller amount of dwarf birch (*Betula nana*), downy willows (*Salix lapponum*), purple marshlocks (*Comarum palustre*), and horsetails (*Equisetum fluviatile*).

From the chamber, a 7 m long FEP inlet (4 mm i.d.) guided 0.25 L min^{-1} of sample air to the CRM setup. A second FEP tube, 20 m long and heated a few degrees above ambient temperature, was used to connect the gas chromatograph-mass spectrometer (GC-MS) to the chamber. The separate inlets were needed as the CRM operates at ambient pressure, which could not be achieved with the pressure drop of the long inlet. At the end of August, adsorbent tubes were used to measure the VOC concentration. These were attached very close to the chamber to avoid sampling line losses (see Fig. 1). A custom-built data logger recorded the temperature and relative humidity (Philips KTY 80/110, Royal Philips Electronics, Netherlands) inside the chamber as well as the photosynthetically active radiation (PAR, LI-190SZ, LI-COR Biosciences, USA) on the top of the chamber (outside).

Comparative reactivity method (CRM)

The instrument used in this study to measure total OH reactivity is described in detail in Praplan *et al.* (2017). It is based on the CRM (Sinha *et al.* 2008), where the OH reactivity of ambient air is measured indirectly via the concentration of a tracer, pyrrole (C_4H_5N). Three measurements of the added, known amount of pyrrole are needed to derive the total OH reactivity: 1) The concentration of pyrrole while diluted in VOC-free air mixed with an OH scavenger and sampled with

the addition of OH (C1); 2) The concentration of pyrrole while diluted in VOC-free air and sampled with the addition of OH (C2); and 3) The concentration of pyrrole while diluted in sample air (containing VOCs) and sampled with the addition of OH (C3).

The OH radicals are created by using a UV lamp ($\lambda < 185$ nm), which photolyzes the water molecules supplied by a nitrogen (purity: 6.0) flow to the reactor arm where the lamp is placed. The VOC-free air for measuring C1 and C2 was created by passing the chamber air through a custom-built catalytic converter, which uses platinum on aluminum pellets (Sigma-Aldrich, USA) heated to 450°C. The pyrrole concentration was measured every 2 min using a gas chromatograph with a photoionization detector (GC-PID, GC955, Synspec B.V., the Netherlands). The measurements alternated every 8 min between C2 and C3, and the first data point after every switch was disregarded. The C2 data were linearly interpolated to match the timing of the individual C3 data points' measurements. Overall, every 16 min a total OH reactivity value was derived. The C2 data were corrected for the relative humidity (RH) difference between C2 (RH_{C2}) and C3 (RH_{C3}) measurements, which is caused by the pump and the custom-built catalytic converter to generate the VOC-free air:

$$C2 = C2_{\text{uncorrected}} - 0.088\text{pptv} \times (RH_{C3} - RH_{C2}). \quad (1)$$

By using the known reaction rate of pyrrole with OH (k_{pyr}, $1.2 \pm 0.18 \times 10^{-10}$ cm^3 s^{-1}, Atkinson *et al.* 1985, Dillon *et al.* 2012), the total OH reactivity of the air in the enclosure can be derived with:

$$R_{\text{meas}} = C1 \times k_{\text{pyr}} \frac{C3 - C2}{C1 - C3} \times D \times A_{\text{PFO}}. \quad (2)$$

The factor D corrected for the dilution of the sample in the reactor and had the value of 1.53. This dilution originates from the nitrogen (purity: 6.0) used to supply water to the UV lamp ($\lambda < 185$ nm) to create the OH radicals.

Additionally, the pseudo-first-order correction factor, A_{PFO}, with the value of 2.32 is used. Equation 2 assumes pseudo-first-order conditions ([Pyrrole] >> [OH]). However, this assumption is not fulfilled, as the mean pyrrole to OH ratio (pyrrole:OH) during the measurements was 2.35 (± 0.41; standard deviation); therefore, a correction must be applied. After the campaign, we calibrated the instrument with isoprene and selected sesquiterpenes to measure the first-order correction factor similar to the one derived by Praplan *et al.* (2020) for α-pinene. For isoprene and a mixture of isoprene and β-caryophyllene, the correction factor was 2.32 (see Fig. S1 in Supplementary Materials).

The total OH reactivity from emissions (TOHRE) is then derived by dividing the R_{meas} by the used flow (f) through, and the area (A_{cham}) of the soil chamber:

$$\text{TOHRE} = \frac{R_{\text{meas}}}{f \times A_{\text{cham}}}. \quad (3)$$

To estimate the limit of detection (LOD) of our setup, Eq. 2 was used, replacing C3 with $C3_{LOD}$:

$$C3_{\text{LOD}} = C2 + 3\sigma_{C2}, \quad (4)$$

where σ_{C2} is the standard deviation of the three 2-minute C2 measurements. Again, $C3_{LOD}$ was linearly interpolated to match the time of the C3 measurements. Finally, Eq. 3 was used to estimate the LOD for the TOHRE. The average LOD for the campaign for all positive values of TOHRE was 0.0086 m s^{-2}.

During periods with very low emissions, especially during nights, C3 can be very close to or even lower than C2, leading to negative R_{meas} and TOHRE values. These can be caused by noise in the measurements or uncertainties of the RH correction. When averaging data of the total OH reactivity from emissions (TOHRE), we did not filter or replace the values under LOD as it would artificially increase the averaged values.

Thermal desorption- gas chromatograph-mass spectrometer (TD-GC-MS)

An online TD-GC-MS was used to measure the emitted VOCs. It consisted of a thermal desorption unit (Turbo Matrix 350) followed by a gas chromatograph (Clarus 680) and a mass spectrometer (Clarus SQ8 T), all manufactured by Perkin-

Elmer, Inc. (USA). It was calibrated using 5-point calibrations with adsorbent tubes containing several VOCs (monoterpenoids (MTs): α-pinene, camphene, β-pinene, Δ-3-carene, *p*-cymene, 1,8-cineol, limonene, myrcene, terpinolene, and linalool; sesquiterpenes (SQTs): longicyclene, isolongifolene, α-gurgunene, β-baryophyllene, β-farnesene, and α-humulene). Unknown SQTs were tentatively identified based on their retention indexes and their mass spectra (Hellén *et al.*, 2020). For isoprene calibrations, a reference gas mixture from National Physical Laboratories was used (32 VOCs at 4 ppb).

At the end of the campaign, samples were collected in adsorbent tubes (Tenax-TA/Carbopack B) for subsequent analysis. Their analysis used the same method; however, another Perkin-Elmer instrument was used, consisting of a TD unit (TurboMatrix 650) connected to a GC (Clarus 600) coupled to a quadrupole MS (Clarus 600 T). Further details about the methods used and measured VOC concentrations can be found in Hellén *et al.* (2020).

The VOC concentrations measured by the GC-MS (VOC_i), as well as their respective reaction rates (k_{VOCi}) were used to obtain the calculated OH reactivity:

$$R_{calc} = \Sigma\, VOC_i \times k_{VOCi}. \quad (5)$$

The calculated OH reactivity emission (COHRE) was calculated by dividing the R_{calc} by the flow (f) through, and the area (A_{cham}) of the soil chamber:

$$COHRE = \frac{R_{calc}}{f \times A_{cham}}. \quad (6)$$

The difference between TOHRE and COHRE is called missing OH reactivity of emissions (MOHRE) in case COHRE is smaller than TOHRE, as additional unknown reactivity is needed to explain the CRM measurements.

Uncertainties of calculations

The uncertainties of the TOHRE were calculated with the following equation (adapted from Praplan *et al.*, 2017):

$$\Delta U_{TOHRE} = \sqrt{\begin{matrix}\Delta U_P{}^2 + \Delta U_S{}^2 + \Delta U_{kOH}{}^2 \\ +\Delta U_D{}^2 + \Delta U_F{}^2 \\ +\Delta U_{PREC}{}^2 + \Delta U_f{}^2\end{matrix}}. \quad (7)$$

The stated uncertainties from Eq. 7, as well as their values, are described below (Table 1). Overall, the relative uncertainty of TOHRE, ΔU_{TOHRE}, is 26%, mainly consisting of the uncertainties of the pyrrole levels (ΔU_p = 12.8%), the uncertainty of the pyrrole reaction rate constant (ΔU_{kOH} = 15%) and the uncertainty of the measurement precision (ΔU_{prec} = 18%).

The uncertainty for COHRE is combined with the measurement uncertainties of the VOC measurements and uncertainties in the reaction rates as well as the flux through the chamber:

$$\Delta U_{COHRE} = \sqrt{\begin{matrix}\Delta U_{VOCi}{}^2 + \Delta U_{kVOCi}{}^2 \\ +\Delta U_f{}^2\end{matrix}}. \quad (8)$$

The ΔU_{VOCi} are described in Hellén *et al.* (2020) and Helin *et al.* (2020) and are between 17% and 30%. One exception is isoprene, which had saturated the selected ion monitoring (mass 67) when the tube samples were collected at the end of the campaign; therefore, the quantification was done using the less sensitive ion scan mode. The normal isoprene uncertainty was doubled for this time (from 20% to 40%) to reflect this. The second source of uncertainty for the COHRE, ΔU_{kVOCi}, comes from the used reaction rates and ranges between 1.5% and 111%. All uncertainties are described below (Table 1). In comparison to ΔU_{TOHRE}, ΔU_{COHRE}'s relative uncertainty varies depending on which VOCs were measured and how large their measured concentrations were. Therefore, the mean values of the uncertainty and the individual ranges are shown (Table 1). While the uncertainties of TOHRE and COHRE used the propagation of error (see Eqs. 7 and 8), the uncertainty of MOHRE was calculated using the min–max method. In this method, the uncertainty of MOHRE is calculated using the highest value for TOHRE (mean TOHRE with maximum error added) and subtracting the lowest COHRE (mean COHRE with maximum error subtracted)

and vice versa. This approach normally leads to larger errors than when the propagation of error method is used.

Results and Discussion

Calculated OH reactivity from the emissions (COHRE)

The VOC emissions from the wetland, described in detail in Hellén *et al.* (2020), were used to derive the COHRE (Fig. 2, Table 2). The earliest measurement period lasted from 25 April until 8 May 2018, during which the chamber sampled the wetland's melting snow cover. The average temperature in the chamber was 3.5°C, and the PAR was 390 μmol m^{-2} s^{-1}. The very low emissions from VOCs trapped in the melting snow led to a very small COHRE of 7.7 × 10^{-6} m s^{-2}. It was dominated by monoterpenoids (91%), while sesquiterpenes contributed with the remaining 9%.

The second period covered 29 May until 4 June 2018, when the snow had melted, and we sampled from Frame 1. The average chamber air temperature was 14°C, and PAR accounted for 540 μmol m^{-2} s^{-1}. This increase resulted in a much higher COHRE of 5.6 × 10^{-3} m s^{-2}, which was dominated by isoprene (76%), followed by SQTs (22%) and MTs (2%).

The third period was 2 days long (6–7 June 2018) and measured from Frame 2 during a cold spell with 7°C and PAR being very low with 290 μmol m^{-2} s^{-1}. The COHRE decreased to 1.7 × 10^{-4} m s^{-2}. Interestingly, this period was dominated by SQTs (81%) followed by isoprene (13%) and MTs (6%). An explanation could be that isoprene emissions are generally known to be mainly light-dependent (Guenther *et al.*, 1995), therefore, the low PAR explains the weak emission of isoprene. However, vegetation differences in the frames could also cause or amplify the lower isoprene emissions.

In the fourth period, from 4–10 July 2018, sampling was done from Frame 1 again. The average temperature in the chamber increased to 20°C, and the average PAR was 560 μmol m^{-2} s^{-1}. Isoprene dominated the COHRE, contributing 89%, followed by SQTs (5%) and MTs (1%). Overall, this period had the second highest COHRE with 1.3 x 10^{-2} m s^{-2}.

The fifth period (12–13 July 2018) used Frame 3. It was the sunniest period with an average PAR of 720 μmol m^{-2} s^{-1}, leading to an average chamber air temperature of 26°C. The COHRE was highest with 2.1 × 10^{-2} m s^{-2} and the isoprene contribution had increased to 93%, followed by SQTs (5%), MTs (1%), and methyl vinyl ketone (MVK, 1%). This is the only period where MVK contributed more than 0.5% of COHRE.

Table 1. Uncertainties related to the TOHRE.

Uncertainty	Relative value (%)	Description
ΔU_{TOHRE}	29.2	overall uncertainty of TOHRE
ΔU_{P}	12.8	uncertainty of pyrrole levels
ΔU_{S}	9.6	uncertainty of pyrrole calibration
ΔU_{kOH}	15.0	uncertainty of reaction rate constant (pyrrole)
ΔU_{D}	2.5	uncertainty of dilution
ΔU_{F}	3.6	uncertainty of fit (first order correction)
ΔU_{prec}	18.0	uncertainty of measurement precision
ΔU_{flow}	5.0	uncertainty of zero airflow through the chamber
ΔU_{σ}	1.9	uncertainty of relative humidity correction
ΔU_{COHRE}	34.7†	overall uncertainty of COHRE (range: 25.1–46.1 %)
ΔU_{VOCi}	22.1*	uncertainty of VOC concentrations (range: 10–40 %)
ΔU_{kVOCi}	28.1*	uncertainty of used OH reactivities (range: 1.5–111 %)
ΔU_{MOHRE}	82.0	overall uncertainty of MOHRE (used min–max approach)

† Average uncertainty over the overlapping period

* Average uncertainty over all measured VOCs.

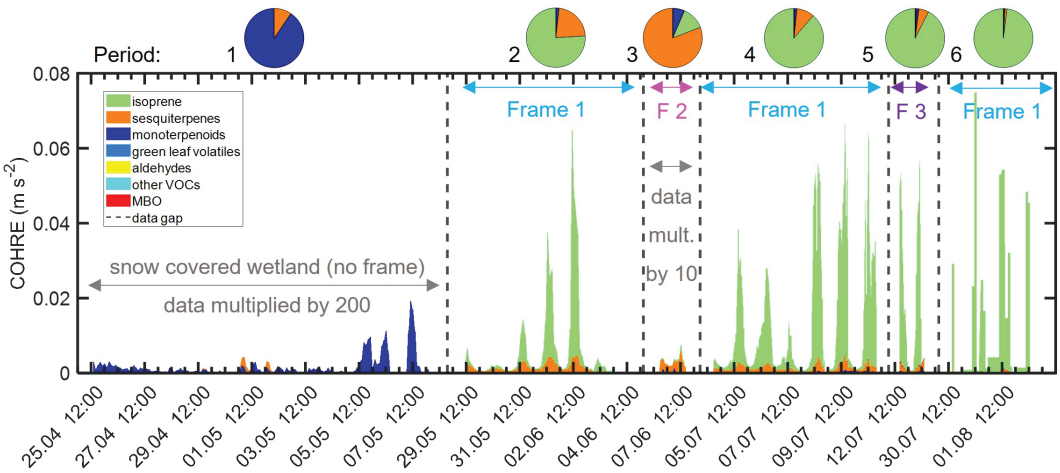

Fig. 2. Overview of the Calculated OH Reactivity Emissions: Measurement periods are separated by vertical black dashed lines. Colorful arrows mark the different chamber frames (= locations) used. Grey arrows mark when the shown data were multiplied by a factor to make it more visible (by 200 in period 1 and 10 in period 3). The pie charts at the top show the composition of the COHRE (values can be found in Table 1). Green leaf volatiles, aldehydes, MBO, and other carbonyls have very low COHRE and are not visible.

The sixth and last period was between 30 July and 2 August 2018. Frame 1 was used, and it was the hottest period with an average chamber air temperature of 30°C, while PAR decreased to 530 µmol m^{-2} s^{-1}. The COHRE was 1.1 x 10^{-2} m s^{-2}, with 98% caused by isoprene and 1% by SQTs. MTs and MVK caused the remaining reactivity.

Overall, the mean COHRE was caused by 89% isoprene, 9% SQTs and 1% MTs, while MVK, green leaf volatiles (GLVs), aldehydes, and other carbonyls contributed less than 1%. After snowmelt, COHRE follows a clear diurnal cycle with maximum COHRE during midday. It peaked on 31 July at 11:12 with 0.075 m s^{-2}.

Table 2. Overview of the Calculated OH Reactivity Emissions. In the case of "-", the compound(s) was/were under our limit of detection. * max PAR is the diurnal (hourly average) maximum PAR of the respective period.

	Period 1	Period 2	Period 3	Period 4	Period 5	Period 6
Start date	25.04	29.05	06.06	04.07	12.07	30.07
End date	08.05	04.06	07.06	10.07	13.07	02.08
Frame	snow	1	2	1	3	1
COHRE (m s^{-2})	7.7 x 10^{-6}	5.6 × 10^{-3}	1.7 x 10^{-4}	1.3 x 10^{-2}	2.0 x 10^{-2}	1.2 x 10^{-2}
isoprene (%)	–	76	13	89	92	98
SQTs (%)	9	22	81	10	5	1
MTs (%)	91	2	6	1	1	< 1
MVK (%)	–	< 1	< 1	< 1	1	<1
GLVs (%)	–	< 1	–	< 1	< 1	–
other VOCs (%)	–	< 1	–	< 1	< 1	–
aldehydes (%)	–	–	–	< 1	< 1	–
T (°C)	3.5	14	7	20	26	30
PAR (µmol m^{-2} s^{-1})	390	540	290	560	720	530
max PAR* (µmol m^{-2} s^{-1})	928	1372	1114	1415	1827	1266
time of max PAR	11:30	13:30	11:30	14:30	13:30	14:30

– indicates the compound(s) was/were under our limit of detection

* indicates the max PAR is the diurnal (hourly average) maximum PAR of the respective period

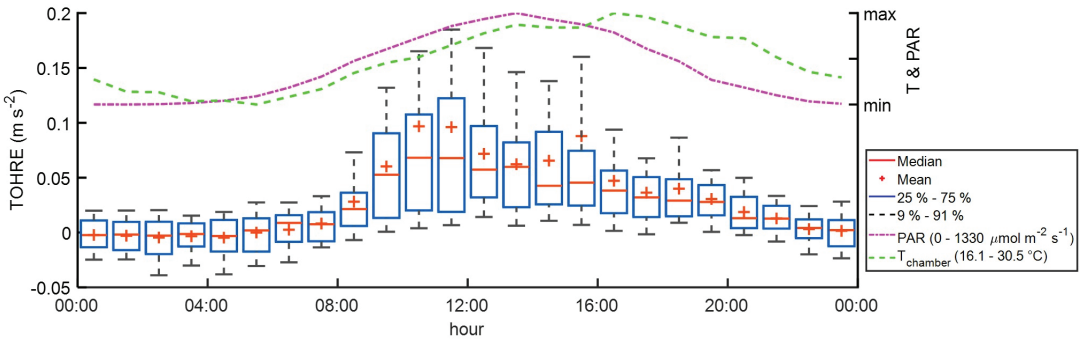

Fig. 3. Diurnal variations of all CRM measurements from the wetland (left axis). The normalized values of PAR and temperature are shown (ranges are stated in the legend) on the right axis.

While COHRE from the boreal trees is dominated by monoterpenes (Praplan *et al.* 2020), the COHRE of this boreal wetland is dominated by isoprene. In earlier wetland emission studies (Haapanala *et al.* 2006, Eckberg *et al.* 2009, Seco *et al.* 2020), isoprene was the main compound emitted and most probably the primary one contributing to COHRE.

Total OH reactivity from the emissions (TOHRE)

The diel pattern of all TOHRE measurements of the wetland followed a clear diurnal peak centered at 11:00–13:00 (Fig. 3) and amounted, on average, to 0.031 m s^{-2}. During the night, the TOHRE values were often under the limit of detection, and, especially from 00:30 to 04:30, the mean and median values were slightly negative. If these negative values are set to zero reactivity, the average daily TOHRE is 0.032m s^{-2}. Starting from 05:30, the TOHRE increases until it peaks before midday, at 10:30, with 0.097 m s^{-2} (median: 0.068 m s^{-2}). The timing of the maximum peak comes as a surprise, as it is clearly earlier than the maxima of the temperature or PAR, which peak at 16:30 and 13:30, respectively. Normally, most biogenic VOC emissions processes follow temperature or PAR. Here, the TOHRE peaks clearly before PAR or temperature, resulting in low correlation coefficients between TOHRE and PAR of 0.49 and between TOHRE and temperature of 0.45. The correlation coefficient of TOHRE and isoprene is 0.47. There can be several explanations for this early maximum; an obvious cause could be primary emissions that the GC-MS did not measure. However, as stated above, the independence of PAR and temperature would be uncommon for biogenic emissions. A second explanation could be that semivolatile VOCs deposit overnight on the colder walls of the chamber and are then released in the morning when the chamber walls are warming up again. A similar process could happen on the water surface; however, the water temperature gradient will be much smaller than the chamber wall's temperature gradient. Additionally, the wetland could start to take up VOCs with increasing temperatures in the afternoon, thereby suppressing their net flux and lowering the OH reactivity. However, with our measurement setup, we could not determine the cause of the early maximum.

A second smaller peak is visible mainly in the mean data at 15:30 with 0.088 m s^{-2}, which is not clearly seen in the median data (0.045 m s^{-2}). The timing of this peak is as expected for biogenic emissions, between the maxima of the temperature and PAR. During this time, the TOHRE varied significantly, which can be seen by the mean value exceeding the 75th percentile. The maximum TOHRE measured during this campaign was also at this time (11 July at 15:29) with 1.2 m s^{-2}. From 16:30, the TOHRE began decreasing, except for a small local maximum in the mean data at 17:30 with 0.040 m s^{-2}. Between 20:00 and 08:00, the mean and median TOHRE were under 0.020 m s^{-2}.

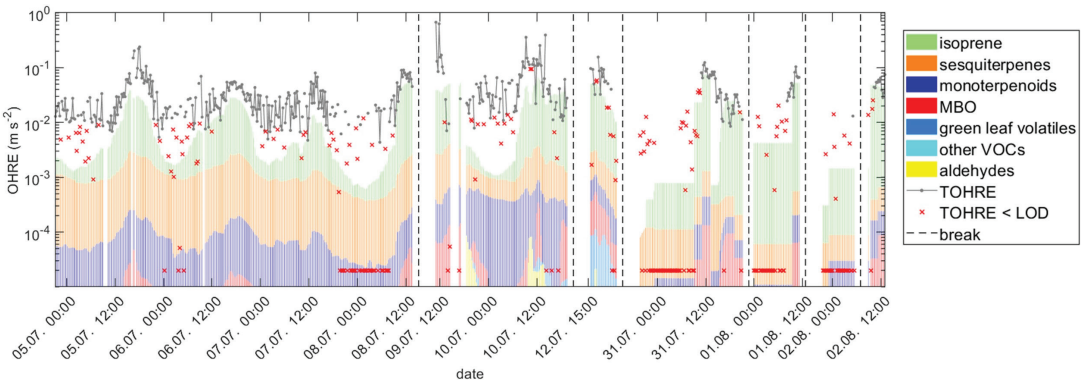

Fig. 4. Comparison between TOHRE and COHRE. TOHRE datapoints which would have been below 10^{-5} m s^{-2} (outside the figure) were added at 2×10^{-5} m s^{-2}.

Missing OH reactivity from emissions (MOHRE)

In this section, only the overlapping measurements of COHRE and TOHRE will be discussed (within the period from 4 July until 2 August; Fig. 4). Even though the COHRE underestimates the TOHRE, both values have a pattern with minima during nights and maxima during the daytime. Overall, only 46% of the TOHRE could be explained (Fig. 5), mainly by isoprene, which contributed to 42% of the TOHRE. Isoprene also showed the highest diurnal variations of all compound classes, with strong emissions during the day and very low emissions during night hours. This behavior differs from the sesquiterpenes, which still showed maximum emissions during the daytime; however, they also had significant emissions during nighttime. This led to interesting situations during nighttime when the COHRE of sesquiterpenes was almost as high as the COHRE of isoprene ($COHRE_{SQT}$:$COHRE_{iso}$ = 0.79) while reaching, on average, only a ratio of less than 0.1. The remaining groups, monoterpenoids, 2-methyl-3-butene-2-ol (MBO), GLVs, other carbonyls, and aldehydes, had a minimal impact on the TOHRE (< 1%). While monoterpenes, MBO, and other carbonyls are constantly emitted, the GLVs and aldehydes were detected only during a short period (8–12 July 2018). The emissions might be related to stress, as many studies linked GLV emissions to plants experiencing stress (Matsui and Koeduka 2016). However, the

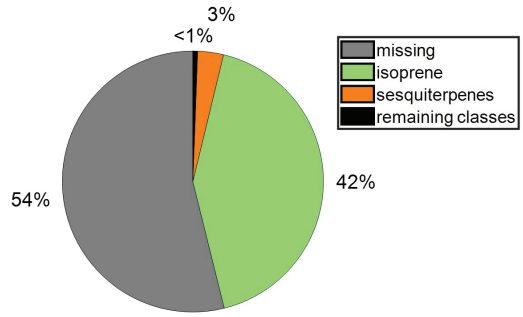

Fig. 5. Closure of the TOHRE, remaining classes includes all classes which contribute less than 1% to the TOHRE.

measured GLVs were under 1% of the COHRE; therefore, we conclude that stress levels were minor and should not have affected the measurements significantly.

The diel average of TOHRE, COHRE and missing OH reactivity from the emissions (MOHRE) show a different pattern and therefore, little correlation with PAR or temperature (Fig. 6). As discussed in the previous section, the early maximum of TOHRE at 11:30 is even more pronounced in this reduced dataset, peaking with 0.094 m s^{-2}. Interestingly, the COHRE has a maximum at 12:30 with 0.038 m s^{-2}, followed by a second peak with 0.029 m s^{-2} at 17:30. It seems that this behavior is unique to our selected period, as in Hellén *et al.* (2020) the emission profiles of isoprene, MTs and SQTs all followed the variations in temperature and PAR.

The MOHRE follows the TOHRE with the highest absolute values during morning and early afternoon and lowest during late

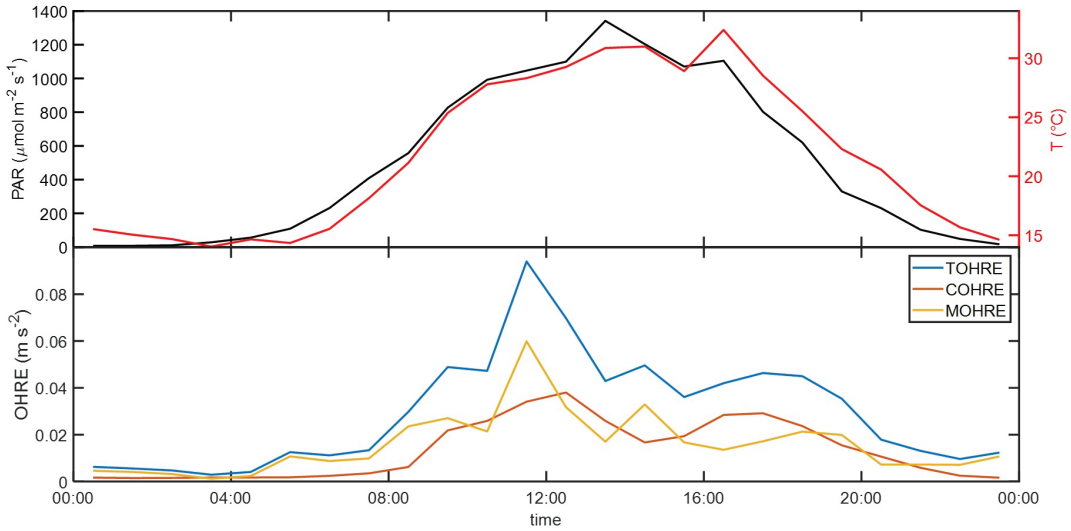

Fig. 6. Diurnal profiles of PAR and temperature (top), as well as Total, Calculated and Missing OH reactivity of emission (bottom).

afternoon and night. The peak was at 11:30 with 0.060 m s^{-2} and the lowest value was at 03:30 with 0.001 m s^{-2}. Interestingly, the relative MOHRE maximum occurs at 23:30 (87%), caused by very low COHRE. The relative MOHRE minimum (32%) was right before the COHRE second maximum at 16:30.

To verify if measurement uncertainties can explain the MOHRE, the time series of TOHRE and COHRE, with their measurement uncertainties, are presented in Fig. 7. In the first half of the campaign, during the daytime, the errors of TOHRE and COHRE rarely overlap, while they do in the campaign's last days (after 30 July). The campaign average values and uncertainties can be seen on the right side, including MOHRE with its uncertainty. The uncertainty of MOHRE was calculated using the min-max approach, so that it can be linked directly to the uncertainties of TOHRE and COHRE.

The uncertainty of MOHRE ranges from 0.003–0.028 m s^{-2}, meaning that the observed MOHRE cannot be fully explained by measurement uncertainties. This leads to the conclusion that our results are caused by emissions we could not detect with our VOC measurements.

To put the average MOHRE of the whole campaign in perspective to VOC emissions, it would need either additionally 0.26 nmol m^{-2} s^{-1} isoprene, 0.49 nmol m^{-2} s^{-1} α-pinene, 0.14 nmol m^{-2} s^{-1} cardinene, or 3.31 nmol m^{-2} s^{-1} ethene to explain the missing reactivity. These additional emissions correspond by a factor of 1.26, 306, and 34 to our campaign's measured isoprene, α-pinene, and cardinene emissions. Ethene was not measured in this study but has been detected in the emissions of a boreal fen (Hellén *et al.*, 2006). However, in that study, the ethene emissions of the boreal fen were clearly lower than isoprene emissions.

Overview of TOHRE studies

A comparison with other studies presenting TOHRE is shown in Table 3. Comparing absolute values (i.e., TOHRE) is not possible, as different methods were used to measure the emission reactivities, leading to results with different units. However, the overview nicely shows the range of MOHRE and the composition of the COHRE and thereby helps to put our results into a broader perspective. To our knowledge, there are three published studies of TOHRE based on CRM measurements, all of which concentrate on tree emissions. In the first, Kim *et al.* (2011) present the overall OH reactivity emissions during

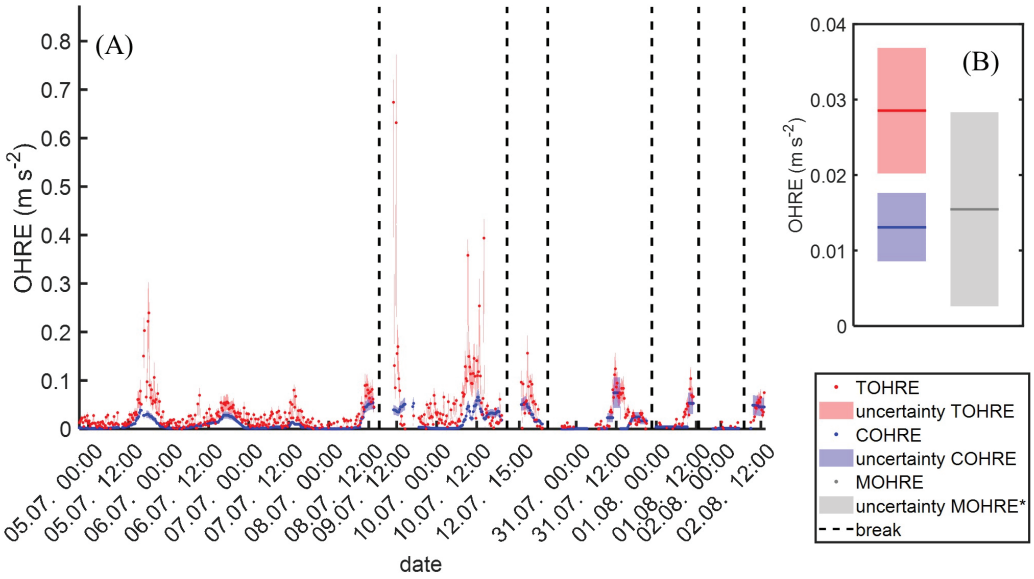

Fig. 7. (**A**) Uncertainty of COHRE and TOHRE during the campaign. (**B**) Campaign averaged TOHRE, COHRE and MOHRE and corresponding uncertainties. *The uncertainty of MOHRE has been calculated using the min–max approach (see Uncertainties of calculations section).

12 days (daytime only) of red oak, white pine, red maple, and beech from a forest in Colorado, USA. They found no significant missing reactivity for the first three tree species and reasonable agreement of COHRE and TOHRE for beech emissions. This study was not added to Table 3, as the results are not expressed in a table, just shown in the figures. Additionally, all presented results from Kim *et al.* (2011) are reactivity values from the chamber, as the conversion to reactivity emissions (dividing the measured reactivity by the flow through the chamber and the dry weight of the branch) was not done.

Nölscher *et al.* (2013) present 49 days of Norway spruce from a stand in Germany. The mean TOHRE was 0.49 s^{-2} g_{dw}^{-1} m^{-3} with 60% MOHRE. The COHRE consisted mainly of monoterpenes (30%), followed by acetaldehyde

Table 3. Overview of previous TOHRE measurements.

	This study Wetland	Nölscher *et al.* (2013) Spruce	Praplan *et al.* (2020) Spruce	Pine	Birch
TOHRE	0.0292	0.49	6.8×10^{-4}	2.0×10^{-4}	14×10^{-4}
(unit)	m s^{-2}	s^{-2} gdw^{-1} m^{-3}	m^3 s^{-2} gdw^{-1}	m^3 s^{-2} gdw^{-1}	m^3 s^{-2} gdw^{-1}
missing	54%	60%	37%	60%	84%
COHRE	46%	40%	63%	40%	16%
isoprene	42%	4%	< 1%	< 1%	< 1%
SQTs	3%	–	16%	6%	6%
MTs	< 1%	30%	28%	29%	5%
MVK	< 1%	–	–	–	–
GLVs	< 1%	–	14%	< 1%	3%
other VOCs	< 1%	–	2%	3%	< 1%
aldehydes	< 1%	–	3%	< 1%	1%
acetaldehyde	–	5%	–	–	–

(5%) and isoprene (4%). Due to the long measurement period, this study shows the variability of the TOHRE and MOHRE nicely over time, as during the beginning of the measurements (spring period), the MOHRE was only 15%, while in the latter half (late summer period) it peaked with 84%.

Praplan *et al.* (2020) present overall emissions during 90 days from Scots pine, Norway spruce, and downy birch seedlings planted in pots and stationed in an opening close to a pine forest in Finland. The mean TOHRE from Norway spruce was 6.8×10^{-4} m^3 s^{-2} g_{dw}^{-1}, and 63% could be explained. The COHRE was dominated by MTs (28%), followed by the SQTs (16%), GLVs (14%), and aldehydes (3%). Isoprene contributed with < 1% and the remaining "other VOCs" with 2% to the TOHRE. The TOHRE measurements of Scots pine averaged $2.0 \cdot x\ 10^{-4}$ m^3 s^{-2} g_{dw}^{-1}, where 60% could not be identified. Leading the COHRE were again the MTs (29%), followed by the SQTs (6%) and isoprene, GLVs, and aldehydes, each < 1%. The remaining "other VOCs" were summed up to 3%. The highest TOHRE, with 1.4×10^{-3} m^3 s^{-2} g_{dw}^{-1}, and the highest MOHRE (84%), were measured from the birch branch. The COHRE (16% of TOHRE) consists of 6% SQTs, 5% MTs, 3% GLV, and 1% aldehydes. Isoprene and "other VOCs" contribute each less than 1%.

In comparison with the above studies, the MOHRE of 54% places this study in the middle range, with results from Kim *et al.* (2011) and the spruce measurements of Praplan *et al.* (2020) being lower, while the MOHRE of pine and birch from Praplan *et al.* (2020), as well as Nölscher *et al.* (2013) exceeding our results. However, all previously published studies in Table 3 have COHRE dominated by MTs or SQTs, while in this study, isoprene is clearly the main contributor. Only Kim *et al.* (2011) have isoprene as the dominating compound in their red oak measurements. The authors state that there was no significant discrepancy between measured and calculated OH reactivity. This concludes that, especially in TOHRE measurements, when oxidation processes are prohibited, the main emitted compound(s) will have minor effects on the MOHRE, as long as they are measured and corrected properly. This leads to the conclusion that in the case of the red oak measurements in Kim *et al.* (2011), isoprene and MTs described the VOC emissions well enough, while they do not in our case of the wetland emissions.

The MOHRE might be caused by a very reactive compound, a large amount of a volatile compound with low reactivity that escapes GC-MS detection, or a substantial number of compounds with low emission rates. Therefore, measurements with a broader array of instruments are needed to detect the sources of MOHRE. State-of-the-art proton transfer reaction mass spectrometers could be especially beneficial to add to GC-MS measurements, as they can measure a greater number of VOCs (however, without being able to separate isomers).

Conclusions

We present for the first time TOHRE from a subarctic wetland in Finland. It is also the first time OH reactivity emission measurements are recorded from vegetation other than a tree branch. The average TOHRE of the campaign is 0.0292 m s^{-2}, and along with the COHRE, followed a diel pattern with higher values during daytime than nighttime. Interestingly, their maxima are before midday and, therefore, before the maxima of PAR and temperature. The source of this behavior could not be identified with our setup. Possible causes could be real primary emissions, not measured by our GC-MS, or deposition and re-emission on chamber walls or the water surface, or a biological update of VOCs by the vegetation during the day.

Overall, 54% of the measured OH reactivity from emissions could not be explained; even when taking measurement uncertainties into account the TOHRE could not be explained by the COHRE. This missing reactivity lies in the mid-tier of previously published OH reactivity emission measurements. However, it is the first time that this high ratio has been seen in an isoprene-dominated ecosystem (due to a lack of publications). The COHRE is dominated by isoprene, which contributes 42% (of TOHRE), followed by the SQTs with 3%. The remaining measured compounds explain less than 1% of the TOHRE. Surprisingly, the SQTs had higher

emissions than the MTs, which can also be seen in the higher COHRE. Due to the measurement setup, we assume that the missing reactivity is caused by primary emissions, as oxidation processes should have no impact in a chamber flushed with air free of VOCs and oxidants.

The heterogeneity of the vegetation in the frames and the wetland, as well as the limited measurement time, make it challenging to upscale the results. Also, VOC concentration measurements on top of the wetland are already dominated by the emissions of the surrounding forests, and isoprene has just a fraction of the ambient monoterpene concentration. However, it is fascinating that wetlands, even though their VOC emissions differ significantly from surrounding boreal forests, still have similar MOHRE fractions (40–60%) to the surrounding trees.

Acknowledgements: The Academy of Finland supported this research (projects 275608, 307797, 314099, 323255, and 307331). The authors thank Timo Mäkelä and Juha Hatakka for their help setting up the measurements and Annalea Lohila for sharing her knowledge of the site (all mentioned work for the Finnish Meteorological Institute). We also like to thank Tarmo Virtanen from the University of Helsinki for identifying the vegetation in the measured frames and Valtteri Hyöky from Metsähallitus for onsite support.

Supplementary Information: The supplementary information related to this article is available online at: http://www.borenv.net/BER/archive/pdfs/ber28/ber28-097-110-supplement.pdf

Data availability: The data shown in the paper is available on request from the corresponding author

References

Atkinson R., Aschmann S.M., Winer A.M. & Carter W.P.L. 1985. Rate constants for the gas-phase reactions of nitrate radicals with furan, thiophene, and pyrrole at 295 ± 1K and atmospheric pressure. *Env. Sci. Tech*. 19, 87–90, doi:10.1021/es00131a010.

Aurela M., Lohila A., Tuovinen J.-P., Hatakka J., Penttilä T. & Laurila, T. 2015. Carbon dioxide and energy flux measurements in four northern-boreal ecosystems at Pallas. *Bor. Env. Res.* 20: 455–473.

Avis C., Weaver A. & Meissner K. 2011. Reduction in areal extent of high-latitude wetlands in response to permafrost thaw. *Nat. Geosci.* 4, 444–448, doi:10.1038/ngeo1160.

Davidson N.C. 2014. How much wetland has the world lost? Long-term and recent trends in global wetland area. *Marine and Freshwat. Res*. 65, 934–941, doi:10.1071/MF14173.

Dillon T.J., Tucceri M.E., Dulitz K., Horowitz A., Vereecken L. & Crowley J.N. 2012. Reaction of Hydroxyl Radicals with C4H5N (Pyrrole): Temperature and Pressure Dependent Rate Coefficients. *J. Phys. Chem. A* 116, 6051–6058, doi:10.1021/jp211241x.

Ekberg A., Arneth A., Hakola H., Hayward S. & Holst, T. 2009. Isoprene emission from wetland sedges, *Biogeosci.* 6, 601–613, doi:10.5194/bg-6-601-2009.

Ferracci V., Heimann I., Abraham N.L., Pyle J.A. & Archibald A.T. 2018. Global modelling of the total OH reactivity: investigations on the "missing" OH sink and its atmospheric implications. *Atmos. Chem. Phys.* 18, 7109–7129, doi:10.5194/acp-18-7109-2018.

Goldstein A.H. & Galbally I.E. 2007. Known and unexplored organic constituents in the Earth's atmosphere. *Env. Sci. Tech*. 41, 1514–1521, doi:10.1021/es072476p.

Haapanala S., Rinne J., Pystynen K.-H., Hellén H., Hakola H. & Riutta T. 2006. Measurements of hydrocarbon emissions from a boreal fen using the REA technique. *Biogeosci.* 3, 103–112, doi:10.5194/bg-3-103-2006.

Helin A., Hakola H. & Hellén H. 2020. Optimisation of a thermal desorption–gas chromatography–mass spectrometry method for the analysis of monoterpenes, sesquiterpenes and diterpenes. *Atmos. Meas. Tech.* 13, 3543–3560, doi:10.5194/amt-13-3543-2020.

Hellén H., Schallhart S., Praplan A.P., Tykkä T., Aurela M., Lohila A. & Hakola H. 2020. Sesquiterpenes dominate monoterpenes in northern wetland emissions. *Atmos. Chem. Phys.* 20, 7021–7034, doi:10.5194/acp-20-7021-2020.

Kaplan J.O., Folberth G. & Hauglustaine D.A. 2006. Role of methane and biogenic volatile organic compound sources in late glacial and Holocene fluctuations of atmospheric methane concentrations. *Glob. Biogeochem. Cyc*. 20, GB2016, doi:10.1029/2005GB002590.

Kim S., Guenther A., Karl T. & Greenberg J. 2011. Contributions of primary and secondary biogenic VOC to total OH reactivity during the CABINEX (Community Atmosphere-Biosphere INteractions Experiments)-09 field campaign. *Atmos. Chem. Phys*. 11, 8613-8623, doi:10.5194/acp-11-8613-2011.

Lelieveld J., Gromov S., Pozzer A. & Taraborrelli D. 2016. Global tropospheric hydroxyl distribution, budget and reactivity. *Atmos. Chem. Phys.* 16, 12477–12493, doi:10.5194/acp-16-12477-2016.

Matsui K. & Koeduka T. 2016. Green Leaf Volatiles in Plant Signaling and Response, in: Lipids in Plant and Algae Development, edited by: Nakamura, Y. and Li-Beisson, Y., Springer International Publishing, 427–443, doi:10.1007/978-3-319-25979-6_17.

Nölscher A.C., Bourtsoukidis E., Bonn B., Kesselmeier J., Lelieveld J. & Williams J. 2013. Seasonal measurements of total OH reactivity emission rates from Norway spruce in 2011. *Biogeosci.* 10, 4241-4257, doi:10.5194/bg-10-4241-2013.

Nölscher A.C., Yanez-Serrano A.M., Wolff S., Carioca de Araujo A., Lavric J.V., Kesselmeier J. & Williams J.

2016. Unexpected seasonality in quantity and composition of Amazon rainforest air reactivity. *Nat. Com.* 7, 10383, doi:10.1038/ncomms10383.

Olefeldt D., Hovemyr M., Kuhn M.A., Bastviken D., Bohn T.J., Connolly J., Crill P., Euskirchen, E.S., Finkelstein S.A., Genet H., Grosse G., Harris L.I., Heffernan L., Helbig M., Hugelius G., Hutchins R., Juutinen S., Lara M.J., Malhotra A., Manies K., McGuire A.D., Natali S.M., O'Donnell J.A., Parmentier F.-J.W., Räsänen A., Schädel C., Sonnentag O., Strack M., Tank S.E., Treat C., Varner R.K., Virtanen T., Warren R.K. & Watts J.D. 2021. The Boreal–Arctic Wetland and Lake Dataset (BAWLD). *Earth Syst. Sci. Data*, 13, 5127–5149, doi:10.5194/essd-13-5127-2021.

Pfannerstill E.Y., Reijrink N.G., Edtbauer A., Ringsdorf A., Zannoni N., Araújo A., Ditas F., Holanda B.A., Sá M.O., Tsokankunku A., Walter D., Wolff S., Lavrič J.V., Pöhlker C., Sörgel M. & Williams J. 2021. Total OH reactivity over the Amazon rainforest: variability with temperature, wind, rain, altitude, time of day, season, and an overall budget closure. *Atmos. Chem. Phys*. 21, 6231–6256, doi:10.5194/acp-21-6231-2021.

Praplan A.P., Pfannerstill E.Y., Williams J. & Hellén H. 2017. OH reactivity of the urban air in Helsinki, Finland, during winter. *Atmos. Env.* 169, 150-161, doi:10.1016/j.atmosenv.2017.09.013.

Praplan A.P., Tykkä T., Schallhart S., Tarvainen V., Bäck J. & Hellén H. 2020. OH reactivity from the emissions of different tree species: investigating the missing reactivity in a boreal forest. *Biogeosci.* 17, 4681–4705, doi:10.5194/bg-17-4681-2020.

Rinne J., Tuovinen J.-P., Klemedtsson L., Aurela M., Holst J., Lohila A., Weslien P., Vestin P., Łakomiec P., Peichl M., Tuittila E.-S., Heiskanen L., Laurila T., Li X., Alekseychik P., Mammarella I., Ström L., Crill P. & Nilsson M.B. 2020. Effect of the 2018 European drought on methane and carbon dioxide exchange of northern mire ecosystems. *Phil. Trans. R. Soc. B*. 375, 20190517, doi:10.1098/rstb.2019.0517.

Seco R., Holst T., Matzen M.S., Westergaard-Nielsen A., Li T., Simin T., Jansen J., Crill P., Friborg T., Rinne J. & Rinnan R. 2020. Volatile organic compound fluxes in a subarctic peatland and lake. *Atmos. Chem. Phys.* 20, 13399–13416, doi:10.5194/acp-20-13399-2020.

Sinha V., Williams J., Crowley J.N. & Lelieveld J. 2008. The Comparative Reactivity Method – a new tool to measure total OH Reactivity in ambient air. *Atmos. Chem. Phys.* 8, 2213–2227, doi:10.5194/acp-8-2213-2008.

Williams J. & Brune W. 2015. A roadmap for OH reactivity research. *Atmos. Env.* 106, 371–372, doi:10.1016/j.atmosenv.2015.02.017.